JOURNAL OF CATALYSIS 112, 528–542 (1988)

$Ba(OH)_2$ as the Catalyst in Organic Reactions

XVIII. Influence of the Microcrystalline Structure and the Nature of Active Sites on Catalytic Activity

J. BARRIOS,* R. ROJAS,† A. R. ALCANRARA,‡ AND J. V. SINISTERRA‡,[1]

*Inorganic Chemistry Department and ‡Organic Chemistry Department, University of Córdoba, Spain, and †Elhuyar Institute, CSIC, Madrid, Spain

Received August 20, 1987; revised March 15, 1988

A detailed study of several barium hydroxide catalysts is made. These basic catalysts are easily obtained from commercial barium hydroxide octahydrate and are studied by thermal analysis, IR spectroscopy, and X-ray powder diffraction techniques. From these studies we can deduce that the most active catalyst, C-200, is β-$Ba(OH)_2$ in the bulk and $Ba(OH)_2 \cdot H_2O$ on the surface. The other catalyst, C-300, consists mainly of α-$Ba(OH)_2$ with a small amount of $Ba(OH)_2 \cdot H_2O$ on the solid surface. The nature and number of active sites are determined by a spectrophotometric method. All the catalysts have reducing and basic sites. The catalytic activity of these solids is tested in Michael addition and in the Wittig–Horner process. The strong basic sites ($pK_a > 11.7$) are responsible for catalytic activity. The structure of adsorbed carbanions is analyzed by IR spectroscopy. This structure differs according to the solid cell lattice where the strong basic site is located.

INTRODUCTION

One of the most important problems in heterogeneous catalysis is how to explain the structure–catalytic activity relationship in order to improve the catalytic process.

The catalytic activity of solid catalysts has been related to the solid structure and to the nature and number of active sites in solid acid catalysts (*1, 2*) and in supported metal catalysts (*3*). The chemical and textural properties of these catalysts can be changed by the addition of alkali metal or fluoride ions (*4, 5*) and these changes are related to the changes in the catalytic activity (*6, 7*).

Similar studies are only in beginning stages in basic catalysis probably because a great many of the basic catalysts described in the literature are air or water sensitive. In this sense, the work carried out on MgO by Szczepanska and Malinowski (*8a,b*) and Matsuda *et al.* (*9*) can be cited.

We have recently described some new barium hydroxide catalysts (*10*) and studied their catalytic activity under interfacial solid–liquid conditions in certain organic reactions of industrial interest, e.g., aldol condensation (*11*), Claisen–Schmidt condensation (*12*), synthesis of Δ^2-pyrazolines (*13*). These new catalysts are more active and selective than commercial ones ($Ba(OH)_2 \cdot 8H_2O$, K_2CO_3, KOH, etc.), under similar experimental conditions (*12–14*).

The catalytic activity of these activated barium hydroxide catalysts has been related to the strong basic sites of the solid, titrated by 4-methyl-2,6-ditertbutylphenol (TBMPHE) (*15*). Nevertheless, a rigorous study concerning the influence of solid microcrystalline structures on the nature of active sites and, so, on catalytic activity, has not been carried out. In the present paper we describe the microcrystalline structure of the catalysts as well as the nature of the active sites and we analyze their influence in two organic reactions of industrial interest.

[1] To whom correspondence must be addressed.

0021-9517/88 $3.00

MICHAEL ADDITION

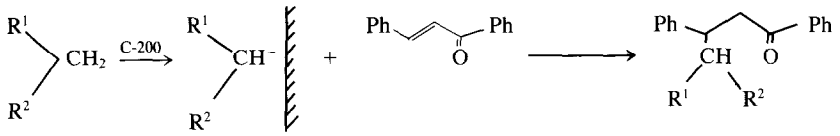

1 adsorbed carbanion **2** **3**

$R^1{=}R^2{=}CO_2Et$

WITTIG–HORNER REACTION

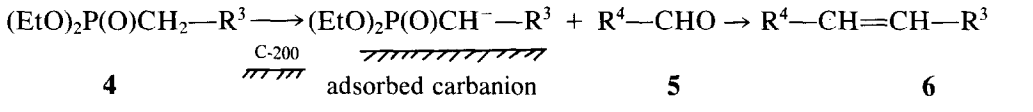

4 **5** **6**

4a $R^3{=}CO_2Et$
4b $R^3{=}CN$

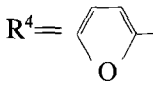

6a $R^3{=}CO_2Et$
6b $R^3{=}CN$

Michael addition is an Ad_N to α,β-unsaturated carbonylic compounds which leads to new carbon–carbon bonds under very mild conditions (*16*). Therefore it is very useful in the synthesis of many drugs and organic compounds of industrial interest (*17, 18*).

The Wittig–Horner reaction is a versatile method for the preparation of α,β-unsaturated esters, **6a** (especially acrylates), and acrylonitrils, **6b**, from aldehydes, **5**. The interest inspired by this reaction explains why so much work has been done on the synthetic aspects of the reaction (*19–21*).

The activated barium hydroxide catalyst C-200 is very active as the basic catalyst for both reactions (*14, 22*). This catalyst leads to better conversions than commercial catalysts ($Ba(OH)_2 \cdot 8H_2O$, K_2CO_3) under similar experimental conditions.

EXPERIMENTAL

Catalyst

The activated barium hydroxide catalysts described in this paper were obtained from commercial barium hydroxide octahydrate (C-0) by 3 h of heating at 200°C (C-200), 300°C (C-300), and 400°C (C-400) in a nickel crucible, according to the method described previously (*10, 22*). The pattern solid melts at 80°C and at 350–370°C during the heating. The color of the catalysts is different: C-200 is white, C-300 is grayish-white, and C-400 is greenish-white. All the calcined catalysts were stored in a closed flask in the presence of NaOH pellets to diminish the rehydration and the adsorption of CO_2.

The surface area was determined by a Carlo-Erba Sorptomatic.

X-ray diffraction diagrams of the stored C-200 and C-300 samples were recorded in a Philips PW 1130 diffractometer using monochromatized Co$K\alpha$ radiation.

TGA and DTA curves were obtained on Staton STA 781 equipment at a 10°C $\cdot$ min^{-1} heating rate, in still and flowing air (50 ml $\cdot$ min^{-1}). About 10 or 25 mg of each sample and 4 mg/10 in. sensitivity were used in each run. Al_2O_3 was the reference material.

The nature and number of catalyst active sites were determined according to a method previously described (*23*). Benzoic

acid, **BA** (pK_a = 4.2), and **TBMPHE** (pK_a = 11.7) were used to titrate the basic sites. 1,3-Dinitrobenzene, **DNB** (EA = 2.2 eV), was used to titrate reducing sites and phenothiazine, **PNTZ**, (IP = 7.31 eV) for the oxidizing ones. Pyridine, **Py** (pK_a = 5.3), and cyclohexylamine, **Cy** (pK_a = 10.6), were used to titrate acid sites.

The millimoles of adsorbed poison (X_m) are related to the number of active sites titrated by the poison (*23*). This value can be used to compare, qualitatively, the number of active sites in each catalyst because the experimental values of X_m are obtained under similar experimental conditions.

Michael Addition Procedure

Chalcone, **2** (25 mmol) is dissolved in 75 ml EtOH (96%). Then, 25 mmol of active methylene compound **1** and 0.5 g of catalyst are added. The mixture is stirred at room temperature for 24 h. Then, the mixture is filtered and washed with hot water to dissolve the catalyst. The solid product, **3**, is not soluble in water.

The reaction yield was determined by dissolving **3** in EtOH. The mixture was analyzed by a Perkin–Elmer Series 2 HPLC using a 5-μC_8 column. P = 1000 psi; $MeOH/H_2O$ = 75/25 (v/v). UV detection occurred at λ = 254 nm. Anthracene was used as the internal standard.

Wittig–Horner Reaction

Triethylphosphonoacetate, **4** (25 mmol), aldehyde, **5** (25 mmol), 2 g of catalyst, 30 ml of 1,4-dioxane, and 0.5 ml of water are successively introduced into a 100-ml flask fitted with a mechanical stirrer and a reflux condenser. The reaction mixture is stirred at 70°C for the reaction time (Table 3). Then, the mixture is filtered and analyzed by GLC using an Intermat I GC 120DFL with a column packed with 5% OVA 101 on Chromosorb W-HMDS 80–60 mesh. Carrier gas is N_2 (1.8 bar). Initial temperature is 140°C. End temperature is 300°C and heating rate is 20°C · min^{-1}.

Selective Poisoning Experiments

The catalyst selective poisoning experiments were carried out following the same procedure already described (*15, 23*). When the poisoning experiment had been carried out, the catalyst was filtered and washed with cyclohexane, Merck p.a. (2 × 5 ml), in order to eliminate the physisorbed poison molecules. The number of unadsorbed poison molecules was measured using a UV–V is spectrometer (Varian, Model Cary 219) in order to find the adsorbed amount of poison.

Then the poisoned catalyst was added to the reaction mixture (see above) and the reaction was determined according to experimental procedure.

IR Spectra of Adsorbed Species

The IR spectra of adsorbed species were recorded by a Perkin–Elmer 599B with a Data Station 3600. The PECDS program was used for the accumulation and differentiation of spectra.

The experimental procedure was as follows. The catalyst, 0.2 g, was added to the solution of the compound to be adsorbed (in EtOH, in Michael addition or in 1,4-dioxane in the Wittig–Horner reaction). The experimental conditions were those described in each experimental procedure.

The mixture was stirred for 5 min to give rise to the adsorption process and to avoid the decomposition of the adsorbed species produced on the solid. The mixture was filtered and washed with 2 × 5 ml of EtOH (99.8% Merck) to eliminate the physisorbed product and the IR spectrum of the solid was recorded.

Trapping Experiments with Merrifield Resin

In order to determine if the carbanion produced from **1** and the ylid from **4**—detected by IR—left the solid surface, Merrifield resin (Ega-Chemie) was used.

The experimental procedure was as follows.

Michael addition. Structure **1** (25 mmol), 25 ml of EtOH (96%), 0.2 g of catalyst, and 1 g of Merrifield resin (1 meq · Cl/g · resin) were mixed and stirred for 48 h (a length of time twice as great as the reaction time). Then, the mixture was filtered and the solid washed with 2 × 10 ml of diethyl ether. The solid was dried under vacuum (100°C) and the IR spectrum recorded.

Wittig–Horner reaction. Merrifield resin (P–CH_2–Cl, 1.0 g) was transformed to the polymer-supported reagent P–CHO by oxidation with DMSO in the presence of $NaHCO_3$ using a method described in the literature (*24*). The main bands of accumulated polymer-supported reagent spectra were 2912, 2844, and 2729 cm^{-1} (CH=O stretching) and 1697 cm^{-1} (conjugated C=O).

Polymer-supported reagent P–CH=O (1 g), 0.4 ml of **1**, 0.05 ml of H_2O, and 1 g of catalyst were stirred at 70°C for 1 h (reaction time 25 min; see Table 3). The mixture was washed with aqueous HCl (20 ml) and acetone. The solid polymer-supported reagent was dried, and the IR spectra were obtained.

RESULTS AND DISCUSSION

Thermal Analysis Studies

In order to determine the composition of each catalyst obtained from commercial barium hydroxide octahydrate (C-0), TGA and DTA curves were obtained (Figs. 1a–1c).

A plateau is observed in the TGA curve of C-0 (Fig. 1a) between 35 and 107°C. Then, a weight loss, which is caused by elimination of seven water molecules (calc. = 39.95%, found = 38.77%) yielding $Ba(OH)_2 \cdot H_2O$ (*25*), which remains stable between 107 and 116°C as shown by the well-defined plateau observed in the TGA curve. This result agrees with those reported in the literature (*26, 27*). Anhydrous β-$Ba(OH)_2$ (*28, 29*) is obtained at 120°C and from this temperature up to at least 370°C no appreciable weight variation occurs in the sample.

The DTA curve shows two endothermic peaks in the temperature range 35–120°C that are caused by the above-indicated dehydration reactions. The smaller endothermic peak appearing between 226 and 246°C must be caused by structural transformation, namely β-$Ba(OH)_2 \rightarrow \alpha$-$Ba(OH)_2$, since no weight variation is observed in the TGA curve. We can deduce that α-$Ba(OH)_2$ is the stable phase at temperatures over 250°C (*29, 30*).

Between 355 and 370°C, α-$Ba(OH)_2$ melts causing the sharp endothermic effect recorded in this temperature interval. This result has been confirmed by visual examination as well as by recording the cooling curve.

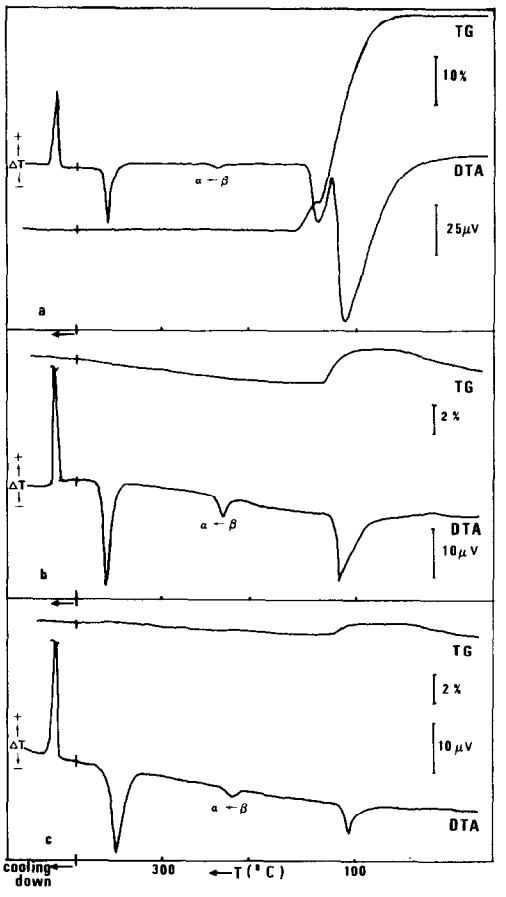

FIG. 1. Differential thermal analysis (DTA) and thermogravimetric (TG) curves of (a) C-0; (b) C-200; (c) C-300 recorded in still air. Heating rate, 10°C · min^{-1}.

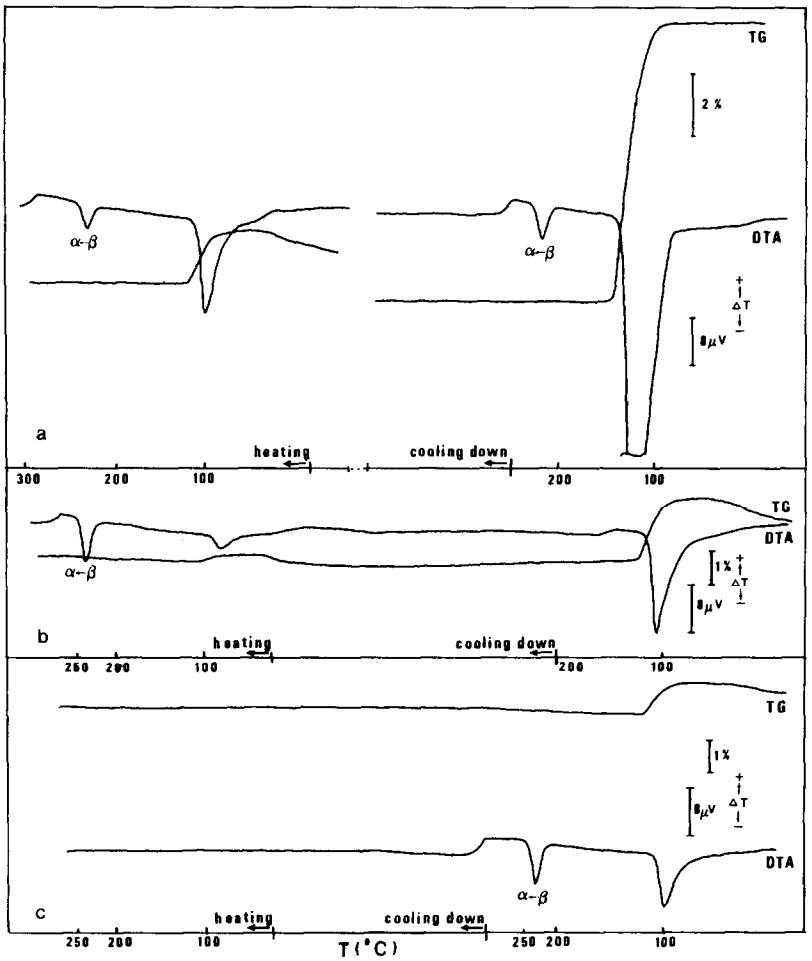

FIG. 2. DTA and TG curves of C-200 recorded (a) after exposure to the air for 3h; (b) after storage on NaOH pellets, still air atmosphere; (c) in flowing air (50 ml · min^{-1}), 10°C · min^{-1} heating rate.

The C-200 catalysts, when obtained, must be anhydrous β-$B(OH)_2$ according to the thermal analysis curves recorded on the C-0 sample. Nevertheless, the TGA curve (Fig. 1b) shows a slight weight increase (1.4%) from room temperature up to 50°C; a plateau exists up to 83°C, which is followed by a step between 83 and 120°C; this corresponds to the endothermic peak observed in the same temperature region. The experimental weight loss for this latest step is 2.1%.

The same behavior is observed for the sample C-300 (Fig. 1c), although the weight variations are considerably smaller.

In order to ascertain the origin of this behavior, several experiments were performed.

C-200 is shown to slightly rehydrate even when stored on NaOH pellets and, consequently, during manipulation. There is very little hydration of C-200 when it is stored in a closed vessel with NaOH pellets for 3 months. Only 2% $Ba(OH)_2 \cdot H_2O$ is detected under these conditions. After exposure to open air for 3 h, C-200 is almost completely transformed into $Ba(OH)_2 \cdot H_2O$, as shown not only by its X-ray diffraction diagram (see next section) but also by the thermograms recorded from this sample in still air atmosphere (Fig. 2a). After 48 h the solid is $Ba(OH)_2 \cdot 8H_2O$.

The weight loss occurring between 100 and 140°C corresponds to the evacuation of 0.9 water molecule (found 0.86). If the sample is cooled in the thermobalance, it partially rehydrates, indicating that the water vapor remaining in the thermobalance enclosure rehydrates the anhydrous compound again.

On the other hand, several batches of C-200 were heated in both still and flowing air atmospheres; the same rehydration–dehydration processes were always observed, but to a smaller extent if thermograms were recorded in a flow of dry air (Figs. 2b and 2c.)

The hygroscopic character of β-$Ba(OH)_2$ as well as the high stability of $Ba(OH)_2 \cdot H_2O$ (*28*) has been reported previously (*29*) and can be explained on the basis of a very high hygroscopicity of the anhydrous hydroxide. Nevertheless, it seems that this rehydration is slow when the solid is stored in a closed vessel in the presence of NaOH (2% $Ba(OH)_2 \cdot H_2O$ in a sample of C-200 after 3 months).

Thermal analysis curves obtained on C-300 under the above-indicated conditions are shown in Figs. 3a and 3b. The rehydration of this sample is considerably lower than that observed for C-200, in both still and flowing air, being practically nonexistent under the above-mentioned experimental conditions.

The TGA and TDA curves of C-400 are qualitatively equal to those previously described for the other two solids. A small water loss at 117°C and a very small peak at 230°C show the presence of traces of $Ba(OH)_2 \cdot H_2O$ in the solid (*11*).

In order to confirm if the weight increases are caused by rehydration rather than by adsorption of CO_2 by the sample, thermograms were recorded on C-300 in dynamic air atmosphere, the air being bubbled through water before going into the thermobalance furnace. In fact, under these

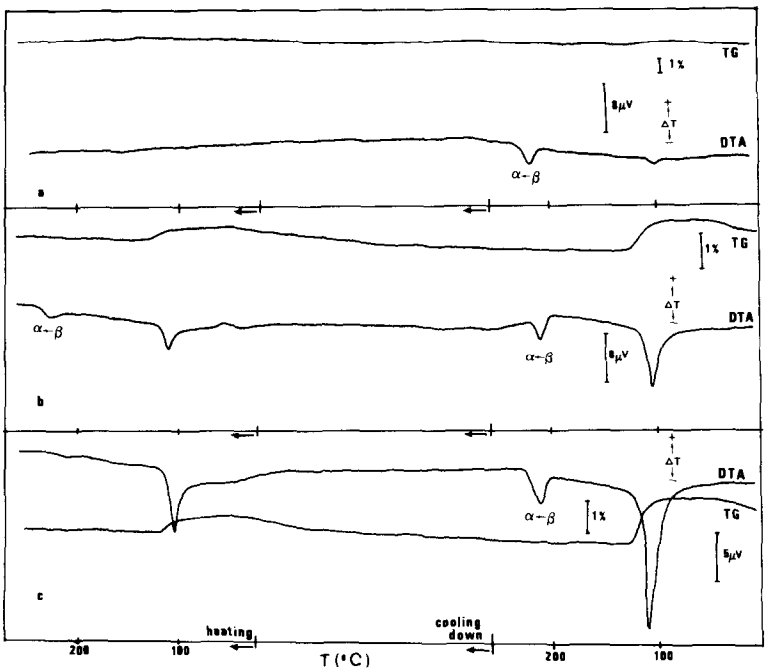

FIG. 3. DTA and TG curves of C-300 recorded (a) in flowing air atmosphere (50 ml · min^{-1}), 10°C · min^{-1} heating rate; (b) in still air; (c) min moist air flow (50 ml · min^{-1}), 10°C · min^{-1} heating rate.

conditions the weight increase and subsequent loss were higher than previously observed (Fig. 3c); $\beta \rightarrow \alpha$ transition also appears at the usual temperature. Nevertheless, in a second heating cycle and although rehydration has occurred (although to a lesser extent), this phase transition is hardly visible in the DTA curve and has practically disappeared when a third heating cycle is carried out, even when rehydration has taken place again.

From all that indicated above, it can be deduced that the equilibra existing in the rehydration–dehydration of the C-200 and C-300 catalysts could be as

$$\beta\text{-Ba(OH)}_2 \rightleftarrows \text{Ba(OH)}_2 \cdot \text{H}_2\text{O}$$
$$\searrow \quad \nearrow$$
$$\alpha\text{-Ba(OH)}_2$$

IR Spectroscopic Analysis

The IR spectra yield information concerning the mode of attachment and the geometry of the water molecules in the crystal lattice. The IR spectrum of the parent compound (C-0; $Ba(OH)_2 \cdot 8H_2O$) shows the presence of a great amount of water (*30, 31*). It shows a broad band at 3450 cm^{-1} which is mainly due to O–H stretching (*32, 33*) in association with intermolecular hydrogen bonding (*34, 35*). The broad bands at 1650 and 1560 cm^{-1} are due to the bending and rocking modes of vibration, respectively (*30*). These facts suggest that the majority of the water molecules of C-0 are trapped in the crystal lattice by weak hydrogen bonds.

The IR spectrum of C-200 confirms these views. The broad band at 3450 cm^{-1} is replaced by two bands: a sharp one at 3580 cm^{-1} characteristic of metal hydroxides (*36, 37*) and a broad one at 2850 cm^{-1} mainly due to hydrogen bonding with a shift to lower frequencies due to decreases in the $OH_2 \leftarrow OH^-$ bond (*36, 37*). From these results we can deduce that the water molecule is weakly bonded to OH^- ions but the other OH^- ions are not H-bonded according to the literature (*36*). Bands at 1680 and 580 cm^{-1} are explained like that of the parent compound C-0. Other bands at 1000 and 850 cm^{-1} are characteristic of several barium compounds (metal–oxygen bond) (*38, 39*). The band at 1450 cm^{-1} could be related to the presence of $BaCO_3$ (1450–1420 cm^{-1} (*30*)). This band shows us that the catalyst is partially carbonated although stored in a hermetically sealed flask in the presence of NaOH. Nevertheless no crystalline $BaCO_3$ was detected by X-ray analysis of the sample recorded at room temperature. So we can say that the CO_2 is adsorbed by means of carbonate bridges or that the $BaCO_3$ produced is amorphous. The adsorption of CO_2 is favored by the temperature according to the increases in weight observed in Fig. 1b ($T > 300$°C) but this fact does not seem to produce microcrystalline barium carbonate, the only species that can be detected by X-ray analysis. Small amounts (<1%) of $BaCO_3$ were detected by other workers in barium hydroxide samples (*30*).

The IR spectra of the stored C-300 and C-400 are similar to that of C-200, so we can say that water is present in both catalysts.

X-Ray Analysis

The X-ray pattern of the initial compound (C-0) agrees with published data for $Ba(OH)_2 \cdot 8H_2O$ (*40*), while X-ray diffraction diagrams recorded on stored C-200 and C-300 catalysts show all lines of β-$Ba(OH)_2$ and α-$Ba(OH)_2$, respectively (*29, 41, 42*), as well as the two most intense diffraction maxims of $Ba(OH)_2 \cdot H_2O$ (*43*) indicating that in both catalysts, some barium hydroxide monohydrate exists. These data corroborate the results obtained from thermal analysis.

$Ba(OH)_2 \cdot 8H_2O$ crystallizes in the monoclinic system (*44*). The barium ions are coordinated by eight water oxygens in the form of a slightly distorted Archimedean antiprism. The OH^- ions are outside the prism (Fig. 4a). The Ba–water molecule distances are 2.69–2.77 Å and the Ba–OH^-, 4.76 and 5.13 Å, respectively

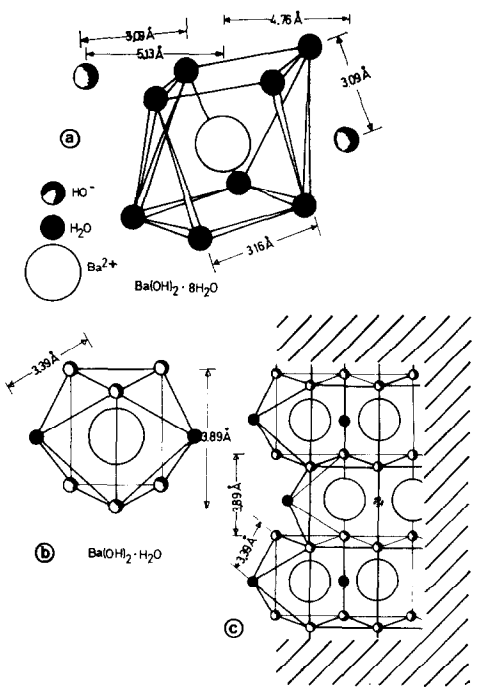

FIG. 4. Ba(II) coordination sphere in (a) $Ba(OH)_2 \cdot 8H_2O$, (b) idem in $Ba(OH)_2 \cdot H_2O$. (c) Structure of surface of $Ba(OH)_2 \cdot H_2O$.

(*44*). The average $OH^- - H_2O$ distance is 3.09 Å (Fig. 4a).

It is well known that $Sr(OH)_2 \cdot H_2O$ and $Ba(OH)_2 \cdot H_2O$ are isostructural, isotypic, and orthorhombic (*45*). On the other hand, β-$Ba(OH)_2$ and $Sr(OH)_2$ are isostructural as well (*46*). The monohydrate is easily produced from β-$Ba(OH)_2$ by a topotactic reaction by hydration with water from the atmosphere. Therefore we can accept that the catalyst used in the reactions (the stored C-200) is β-$Ba(OH)_2$ in the bulk and $Ba(OH)_2 \cdot H_2O$ on the surface. In the hydrate each Ba(II) is coordinated to six OH^- and two water molecules (Fig. 4b). The structure of the C-200 surface is shown in Fig. 4c where the average $OH^- - H_2O$ in $Ba(OH)_2 \cdot H_2O$ is 3.39 Å.

This $Ba(OH)_2 \cdot H_2O$ structure is present in stored C-300 in a very small amount (empirical formula from TGA $Ba(OH)_2 \cdot H_2O$, 0.06 H_2O). Therefore stored C-300 is α-$Ba(OH)_2$ and a very small amount of $Ba(OH)_2 \cdot H_2O$ is on the surface (produced by rehydration of α-$Ba(OH)_2$ according to the TGA and TDA curves).

The coordination sphere of Ba(II) and the average distances $OH^- - OH_2$ from $Ba(OH)_2 \cdot 8H_2O$ and $Ba(OH)_2 \cdot H_2O$ obtained from the literature data (*44–46*) are shown in Fig. 4.

The C-400 X-ray analysis was not carried out due to the instability of this green solid that turns greenish-white on contact with the atmosphere.

Nature and Numbers of Active Sites

The surface area of solid catalysts and the nature and number of active sites of solids are shown in Table 1. The low surface area values are due to the microcrystalline structure of the solid. All the values are very similar within experimental error. Therefore, the surface area is not a property that can explain the catalytic activity of these solids.

All the catalysts have only basic and reducing sites. No acid sites versus pyridine (**Py**) or cyclohexylamine (**Cy**) and no oxidizing versus phenothiazine (**PNTZ**) are present in the catalyst. This result agrees with the nature of Ba(II) which does not have a strong acid or oxidant character.

The number of strong basic sites titrated by **TBMPHE** ($pK_a = 11.7$) is greater in C-0 than in other cases. Nevertheless, due to the high amount of water H-bonded in this catalyst (see IR section), the value obtained seems not to be significant. Probably the titration of active sites takes place at the same time as the dehydration and demolition of the cell lattice because a slight dissolution of the C-0 is observed in this case. This fact could explain the high value obtained.

In the other catalysts, the obtained values are

$$\text{C-200} > \text{C-300} > \text{C-400}.$$

These active sites are mainly responsible for the catalytic activity of the activated

TABLE 1

Chemical and Textural Properties of Activated Barium Hydroxide Catalyst

	C-0	C-200	C-300	C-400
Surface area (m^2/g)	1.4 ± 0.1	1.9 ± 0.1	1.4 ± 0.1	1.2 ± 0.1
Number of active sites (μmol/g · cat)				
TBMPHE (pK_a = 11.7)	260 ± 50[a]	6.3 ± 0.2	2.2 ± 0.2	0.6 ± 0.1
BA (pK_a = 4.2)	—[b]	80 ± 10	60 ± 10	56 ± 10
DNB (EA = 2.21 eV)	55 ± 6	28 ± 3	13 ± 3	15 ± 3
PNTZ (IP = 7.13 eV)[c]	—	—	—	—
Py (pK_a = 5.3)[c]	—	—	—	—
Cy (pK_a = 10.6)[c]	—	—	—	—

[a] The solid is slowly dissolved by the TBMPHE.

[b] No adsorption equilibrium is reached. The solid is slowly dissolved by the cyclohexanic solution of Ba.

[c] No adsorption was determined.

barium hydroxide catalyst in Michael addition (*15*). These active sites must be related to unhindered superficial OH^- whose negative charge is not compensated by the Ba(II) from the lattice. Due to the fact that $Ba(OH)_2$ is on the solid surface, the strong basic site could be the external OH^- of the cube H-bonded to the water.

Total basicity of the catalyst can be determined by titration with **BA**, the obtained values being

$$\text{C-200} \approx \text{C-300} \approx \text{C-400}$$

within experimental error. Therefore the number of basic sites of C-0 versus **BA** cannot be determined due to the dissolution of the solid.

The number of reducing sites versus DNB is

$$\text{C-0} > \text{C-200} > \text{C-300} > \text{C-400}.$$

The nature of these sites could be (i) negative charge zones produced by two neighboring microcrystals (*47, 48*) or (ii) O^{2-} produced during the calcination process. The first sites would be one-electron donor sites responsible for the catalytic activity of C-200 in the Cannizzaro reaction under ultrasound (*49*). The second kind of site would be basic and reducing sites.

Catalytic Activity

Michael addition. The results obtained in the Michael addition of diethylmalonate, **1**, to chalcone **2**, catalyzed by C-0, C-200, and C-300 are shown in Table 2. The C-400 catalyst did not catalyze the process.

From these data we can say that C-200 is the most active catalyst (entry 1 versus 4 and 7). This fact cannot be related to the surface area because the values are similar in all cases (Table 1).

The catalytic activity of C-200 versus C-300 could be explained by the greater amount of strong basic sites without steric hindrance (titrated by the **TBMPHE**) in C-200 than in C-300. These active sites have very little steric hindrance because they are titrated by the bulky **TBMPHE** molecule. So, the bulky molecules **1** and **2** could react on this catalytic site because steric hindrance cannot prevent the reaction. On the other hand the $pK_a > 11.7$ of these sites is similar to the pK_a of **1** (pK_a = 12.7). Therefore, the basicity of these sites would be valid for carrying out the formation of carbanion from **1**. This statement agrees with the selective poisoning data (Table 2, entries 1 versus 3 and 4 vs 6), where the poisoning of these sites produces null conversions.

TABLE 2

Selective Poisoning Experiments of Active Sites in Michael Addition of **1** to **2**

Entry	Catalyst	Kind of active site (poisoning agent)	Number of active site (μmol/g · cat)	Amount of adsorbed poison (μmol/g · cat)	Yield in **3** (% molar)[a]
1	C-200	—	—	—	95
2	C-200	Reducing (**DNB**)	28 ± 3	30 ± 3	58
3	C-200	Basic (**TBMPHE**)	6.3 ± 0.2	6.7 ± 0.3	5
4	C-300	—	—	—	52[b]
5	C-300	Reducing (**DNB**)	13 ± 3	14 ± 1	2
6	C-300	Basic (**TBMPHE**)	2.2 ± 0.2	2.8 ± 0.3	5
7	C-0	—	—	—	80[b]
8	C-0	Reducing (**DNB**)	55 ± 6	53 ± 5	0
9	C-0	Basic (**TBMPHE**)	260 ± 50	268 ± 60[c]	0
10	C-400	—	—	—	2

Note. T = 25°C; t. react. = 24 h; 0.2 g · cat.: solvent EtOH (96%); 25 mmol of **1** and **2**.

[a] Error ±5%.

[b] C-0 catalyst, 0.5 g versus 0.2 g, in the case of C-200 and C-300.

[c] The solid is partially dissolved.

Commercial barium hydroxide, C-0, is less active than C-200 because a lower yield is obtained with 0.5 g of C-0 versus 0.2 g in the case of C-200 (entry 7 vs 1, Table 2). As in the other cases, the selective poisoning of the active sites titrated by **TBMPHE** leads to null conversions.

Therefore, the number of strong basic sites cannot only explain the relative catalytic activity of C-0 and C-200. It is necessary to assume that the microcrystalline structure of the solid and the amount of water play a very important role in catalytic activity. This is discussed in the analysis of adsorbed species.

The role of reducing sites (titrated by **DNB**) is different. In the case of C-200 there is a small reduction in the yield when these sites are poisoned (entry 2 vs 1, Table 2). Therefore, we can say that these active sites in C-200 are not responsible for the catalytic activity in this reaction for the most part. Therefore, the strong basic sites acting in the process are not reducing ones. They must be OH^-. These OH^- are probably from superficial $Ba(OH)_2 \cdot H_2O$ (Fig. 4b).

When the reducing sites of C-300 and C-0 are poisoned, null conversions are obtained. This can be explained by the fact that the reducing sites in these catalysts are basic and reducing.

Both kinds of active sites have been described by Tanabe *et al.* for other basic solids (*47, 48*). The one-electron donor sites are produced by two neighboring microcrystals and are more abundant in solids with small cell lattices than in solids with large ones. So C-200 (practically $Ba(OH)_2 \cdot H_2O$ on the surface), with smaller cell lattices than C-300 (practically α-$Ba(OH)_2$) and C-0 ($Ba(OH)_2 \cdot 8H_2O$), will have pure one-electron donor sites (no basic sites). So, **DNB** poisoning cannot prevent basic catalysis.

The reducing basic sites are O^{2-} (*47, 48*) produced by dislocation of the cell lattice and they are abundant in solids with the large C-0 and C-300 cell lattices. This fact could explain why **DNB** poisons these catalysts in Michael addition but not in the case of C-200.

Wittig–Horner reaction. Similar conclusions can be obtained from the Wittig–Horner reaction (see Table 3).

In the synthesis of acrylates, **6a**, we can

TABLE 3

Selective Poisoning Experiments in the Wittig–Horner Reaction

Entry	Compound	Catalyst	Kind of active site (poisoning agent)	Number of active sites (μmol/g · cat.)	Amount of adsorbed poison (μmol/g · cat.)	Yield in 6[a] (% molar)/t(min)
1	**6a**	C-200	—	—	—	100/25
2	**6a**	C-200	Reducing (**DNB**)	28 ± 3	32 ± 3	88/25
3	**6a**	C-200	Basic (**TBMPHE**)	6.3 ± 0.6	6.2 ± 0.3	2/25
4	**6a**	C-300	—	—	—	32/30
5	**6a**	C-300	Reducing (**DNB**)	13 ± 3	14 ± 1	0/30
6	**6a**	C-300	Basic (**TBMPHE**)	2.2 ± 0.2	3.0 ± 0.3	5/30
7	**6a**	C-0	—	—	—	61/30
8	**6a**	C-0	Reducing (**DNB**)	55 ± 6	54 ± 7	0/30
9	**6a**	C-0	Basic (**TBMPHE**)	260 ± 50	268 ± 60	0/30
10	**6b**	C-200	—	—	—	100/40
11	**6b**	C-200	Reducing (**DNB**)	28 ± 3	30 ± 4	80/40
12	**6b**	C-200	Basic (**TBMPHE**)	6.3 ± 0.6	6.4 ± 0.6	2/40
13	**6a**	C-400	—	—	—	3/180
14	**6b**	C-400	—	—	—	0/180

Note. 1,4-Dioxane, 30 ml; T = 70°C; 2.5 g · cat; Furfural = 0.02 mmol; **4a** or **4b** = 0.025 mmol.
[a] Error ±5%.

see that C-200 is the most active catalyst (entry 1 versus 4 and 7, Table 3). On the other hand, the C-200 catalyst improves the reaction versus such other catalysts as K_2CO_3 (*14*) under the same experimental conditions. A more detailed discussion from a synthetic point of view was given in a previous paper (*14*).

The catalytic activity is

$$\text{C-200} > \text{C-0} > \text{C-300}$$

as in Michael addition (see above). This different catalytic activity cannot be related to the surface area, which is similar in all cases (Table 1).

The number of strong basic sites titrated by **TBMPHE** with $pK_a > 11.7$ (similar to phosphonoacetate ($pK_a = 12.2$ (*50*)) cannot explain this fact, because the most active catalyst, C-200, has fewer strong basic sites titrated by **TBMPHE** than C-0. Nevertheless they are responsible for the catalytic activity in this process as can be deduced by selective poisoning experiments (entries 3, 6, and 9, Table 3).

When the reaction is carried out with anhydrous 1,4-dioxane, and C-200, lower reaction yields are obtained (20%) (*14*) than when slightly hydrated 1,4-dioxane is used as the solvent (Table 3, entry 1). An X-ray diffraction diagram of the solid obtained from the reaction in anhydrous solvent showed that this solid was pure β-$Ba(OH)_2$ (*51*). So, the catalytic activity must be related to the presence of strong basic sites in *a specific cell lattice with a specific geometric and steric structure*. This is discussed in the next section.

The catalytic role of reducing sites is similar to that described in Michael addition.

The synthesis of acrylonitrils, **6b**, is even poorer than the synthesis of acrylates because longer reaction times are necessary to obtain poor yields. As in the synthesis of acrylates, the strong basic sites are responsible for the catalytic activity (see Table 3).

The C-400 cannot catalyze the process.

Detection of Adsorbed Species on Solids

The structure of adsorbed species from **1** on solids (C-0, C-200, and C-300) was studied by IR spectra of the solids after contact (under reaction conditions) with the precursors of the carabanions, **1, 6a,** or **6b.** The PECDS program was used for the accumulation and manipulation of spectra.

Michael addition. When the ethanolic solution of **1** and the solid catalyst are put together under reaction conditions for some

minutes (see Experimental), and the mixture is filtered, only those IR bands like **1** are observed in the liquid in all cases.

On the other hand, when we record the IR difference spectra of solids we obtain different IR absorptions. These absorptions could be related to adsorbed species more conjugated than **1**. These bands are the following:

1735 cm^{-1} CO–OEt (slightly conjugated) but 1740 cm^{-1} for **1**.

1600–1550 cm^{-1} broad band with two maxims:

1500 and 1550 cm^{-1}, related to C=O B_{1u} (1578 cm^{-1} (*51*)) and C=C=C B_{2u} (1527 cm^{-1} (*51*)) vibrations.

1390 and 1290 cm^{-1} (weak). They can be related to C=O B_{2u} (1397 cm^{-1} (*48*)) and C=C=C B_{1u} (1218 cm^{-1} (*51*)) vibrations.

Therefore we can postulate **7** as the structure for carbanion from **1**, adsorbed on the $Ba(OH)_2 \cdot H_2O$ cell lattice. In this case there are two different C=O bonds: one slightly conjugated (1735 cm^{-1}) and the other very conjugated (1580 cm^{-1}).

This can be explained by the fact that the process takes place in the strong basic sites. In these sites there is a distance $OH^- - H_2O$ = 3.39 Å, related to the $Ba(OH)_2 \cdot H_2O$ structure (Fig. 5), similar to the distance of the enolate ion, **7**, 2.9 Å. Therefore carbanion can be produced on this site because the geometrical and steric characteristics (two oxygens at 2.9 Å) are similar to those of the active sites (two oxygens at 3.39 Å).

Chalcone is not adsorbed on the solids. Therefore a mechanism like that proposed in Fig. 5 could be postulated for the process where the adsorbed carbanion reacts with the chalcone from the liquid phase.

A similar IR spectrum was recorded in the case of C–0. Therefore we must deduce that **7** is produced on the active site of C-0, also. The process takes place in the strong basic sites (Table 2). The active sites in this catalyst could be the OH^- placed at 3.09 Å of the water molecule in the barium hydroxide octahydrate structure (Fig. 4a). Therefore we have a distance and structure similar to those in $Ba(OH)_2 \cdot H_2O$. The poor yields obtained can be related to the presence of a great number of water molecules near **7** that are acid versus the carbanion. Therefore, they can react with **7** giving **1**, diminishing the number of carbanion produced and, so, diminishing the yield.

In the case of C-300, 1735 cm^{-1} was not present. Therefore we can say that a more conjugated species is produced in this case with a slight carbanionic character in the CH that explains the poor yields obtained. The formation of this species is related to the α-$Ba(OH)_2$ (main compound of C-300). Unfortunately we do not have the α-$Ba(OH)_2$ structure to discuss qualitatively the structure of the adsorbed carbanion.

The Michael addition takes place under interfacial solid–liquid conditions because the carbanion from **1** is not trapped by Merrifield resin (P–CH_2Cl 1 meq/g). This is shown by the IR spectra of the resin where the 1740 cm^{-1} from **CO**–OEt is not observed when the polymer is mixed with the catalyst and **1** under the reaction conditions for 24 h,

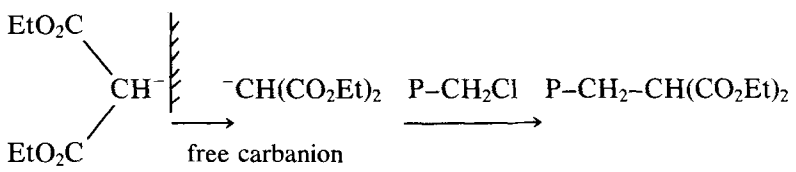

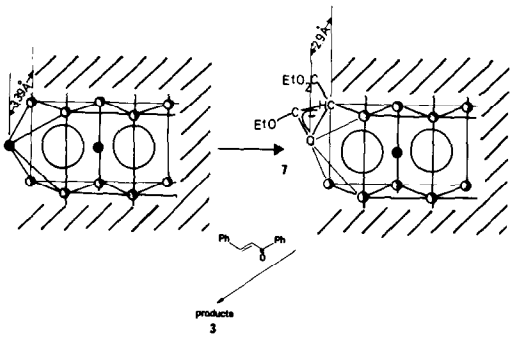

FIG. 5. Carbanion from diethylmalonate adsorbed on $Ba(OH)_2 \cdot H_2O$ (on the surface of C-200 catalyst), **7**.

Therefore we can say that carbanion remains adsorbed on the solid surface and the process is an interfacial solid–liquid mechanism. This behavior is similar to that described for other organic reactions catalyzed by C-200, e.g., aldol condensation (*11*).

Wittig–Horner reaction. The nature of the adsorbed species produced in the adsorption of **4a** on the catalysts was analyzed by IR spectroscopy (Table 4).

The IR spectrum of the adsorbed species on C-200 shows a 1670 cm^{-1} band related to the C=O vibration mode of a very conjugated ester (*52*). The adsorption at 1592 and 1384 cm^{-1} is related to a conjugated C=C bond. There is no P → O band detected although a 1194 cm^{-1} band can be related to P=O. All these absorptions are justified by comparison to similar structures for the *Z* form of ylid salt described for K(I) and Li(I) (*53, 54*).

On the other hand, the distance O_6–O_5 is 3.35 Å, very similar to the OH^-–H_2O distance in the barium hydroxide monohydrate structure, 3.39 Å (Fig. 4b). Therefore we can describe the adsorbed species as **8** (see Fig. 6) where the negative oxygen is placed where the OH^- had been in the lattice. Therefore an interaction with the $5d^0$ of Ba(II) is present and so, the P → O is relaxed. The presence of 1570 and 1670 cm^{-1} absorption shows a delocalization of the negative charge in the ylid, with a

TABLE 4

Main IR Bands (cm^{-1}) of Diethyl-(carboethoxymethylen)-phosphonate, 4a, and Those of the Adsorbed Species on Catalysts

		Adsorbed Species from **4a** on		
	4a	C-200	C-300	C-0
$\alpha(C_2{=}O_5)$	1740	—	—	—
$\alpha(C_2{=}O_5)$	—	1670	—	1675
$\alpha(C_1{=}C_2)$	—	1570	—	1568
$\alpha(C_1{=}C_2)$	—	1384	1384	1384
$\alpha(P \rightarrow O_6)$	1275	—	1259	—
	1210	—	1210	—
$\alpha(P{=}O_6)$	—	1194	—	1194
$\alpha(C_2{-}O_3)$	1120	1112	1115	1090

negative character in C_1. This negative charge explains the high reactivity observed in this Wittig–Horner reaction. The fact that the O_5–O_6 distance (3.35 Å in **8**) is very close to the distance of the cell lattice (3.39 Å) could explain why the Wittig–Horner reaction takes place more quickly (25 min) than Michael addition (24 h) when the distance in **7** is 2.9 Å.

When the adsorbed species on C-0 and C-300 are compared to that on C-200, we observe that the adsorbed species on C-0 and C-200 may be similar (similar IR bands). This fact can explain why the catalytic activity of C-0 is higher than that of C-300. These similar structures can be explained by the presence of the distance OH^{-1}–H_2 = 3.09 Å (Fig. 4) in the barium hydroxide octahydrate, similar to the distance between the O_6 and O_5 in the ad-

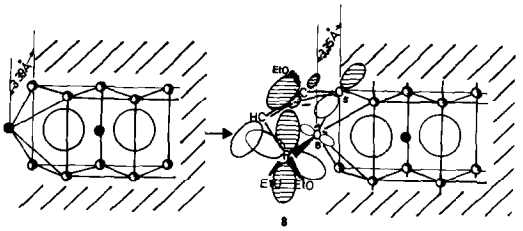

FIG. 6. Ylid from **4a** adsorbed on $Ba(OH)_2 \cdot H_2O$ (on the surface of C-200 catalyst), **8**.

sorbed ylid (3.35 Å) and to the OH^-–H_2O distance in the $Ba(OH)_2 \cdot H_2O$. Nevertheless, C-0 is less active than C-200 (Table 3 entries 7 vs 1). This fact can be explained only by the presence of a great amount of water in the C-0 ($Ba(OH)_2 \cdot 8H_2O$) which acts as an acid versus the ylid breaking it up.

The adsorbed species on C-300 has the P → O band like **4a** but not the **CO**–OEt band. Therefore we are led to think that, in this case, P → O_6 is not bonded to the cell lattice of α-$Ba(OH)_2$ (the main component of the solid). C=O_5 is not present but C_1=C_2 is. Therefore we must postulate a different structure for the adsorbed species on C-300.

In this case the negative charge is over the O_5. Therefore the C_1H is less negative than in the case of C-0 and C-200. This explains the low reactivity observed in C-300.

When the adsorption of **4b** is carried out on C-200, the presence of CN absorption (2259 cm^{-1} in **4b**) is not observed although there is a small band at 1690 cm^{-1} that could be related to the C=N bond of the carbanionic species **9**. The 1150 cm^{-1} absorption could be related to P=O_6. Therefore, **9** could be postulated as the adsorbed ylid. This species has been described previously as the reaction intermediate (*55*) and adsorbed on K_2CO_3 catalyst (*50*). It is evident that geometrical factors and the poor affinity of N for the Ba(II) discourage the adsorption and make **9** more unstable than **8**. In Fig. 7 we can say that the N–O distance (3.72 Å) is greater than that of water–OH^- in $Ba(OH)_2 \cdot H_2O$ (3.39 Å). These facts qualitatively explain the poor yields obtained in the synthesis of **6b**.

As in the case of Michael addition, no trapping of the ylid by the polymer-supported reagent (P–CHO) was observed in any case because the ester band **CO**–OEt (1740 cm^{-1}) or that of CN (2259 cm^{-1}) was not observed in the IR spectra of the resin after the reaction with the adsorbed ylid.

This fact confirms that all the processes studied are interfacial reactions. In these cases the structure of the basic catalysts controls the process by means of the structure of the adsorbed carbanion.

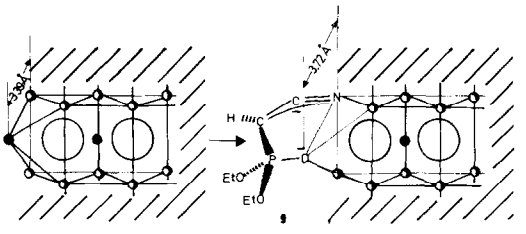

FIG. 7. Ylid from **4b** adsorbed on $Ba(OH)_2O$ (on the surface of C-200 catalyst), **9**.

REFERENCES

1. Aramendia, M. A., Borau, V., Jimenez, C., Marinas, J. M., and Rodero, F., *Colloid Surf. Sci.* **70,** 209 (1977).
2. Cheung, T. T. P., Willcox, K. W., McDaniel, M. P., and Johnson, M. M., *J. Catal.* **102,** 10 (1986).
3. Aramendia, M. A., Borau, V., Gomez, J. F., Jimenez, C., and Marinas, J. M., *React. Kinet. Catal. Lett.* **30,** 329 (1986).
4. Figoli, N. S., Hillar, S. A., and Parera, M., *J. Catal.* **20,** 230 (1971).
5. Grabowski, W., and Malinowski, S., *Bull. Acad. Pol. Sci.* **24,** 843 (1976).
6. Campelo, J. M., Garcia, A., Gutierrez, J. M., Luna, D., and Marinas, J. M., *J. Colloid Interface Sci.* **102,** 107 (1984).
7. Scokart, P. O., Selim, S. A., Damon, J. P., and Rouxhet, P. G., *J. Colloid Interface Sci.* **70,** 209 (1977).
8. (*a*) Szczepanska, S., and Malinowski, S., *J. Catal.* **15,** 68 (1969); (*b*) **27,** 1 (1972).
9. Matsuda, T., Sasaki, K., Miura, M., and Sugiyama, K., *Bull. Chem. Soc. Japan* **58,** 1041 (1985).
10. Garcia-Raso, A., Sinisterra, J. V., and Marinas, J. M., *Polish J. Chem.* **56,** 1435 (1982).
11. Barrios, J., Marinas, J. M., and Sinisterra, J. V., *Bull. Soc. Chim. Belg.* **95,** 107 (1986).
12. Sinisterra, J. V., Garcia-Raso, A., Cabello, J. A., and Marinas, J. M., *Synthesis,* 502 (1984).
13. Sinisterra, J. V., *React. Kinet. Catal. Lett.* **30,** 93 (1986).
14. Sinisterra, J. V., Mouloungui, Z., Delmas, M., and Gaset, A., *Synthesis,* 1097 (1985).
15. Sinisterra, J. V., Garcia-Blanco, F., Iglesias, M., and Marinas, J. M., *React. Kinet. Catal. Lett.* **27,** 263 (1985).

16. Hoppmann, A., Weyerstahl, P., and Zummack, W., *J. Liebig Ann. Chem.* **9,** 1547 (1977).
17. Joworski, T., Kolodzeiejek, W., Prejzner, J., and Wlostowski, M., *Polish. J. Chem.* **55,** 1321 (1981).
18. Fang, J. M., *J. Org. Chem.* **47,** 3464 (1982).
19. Becker, K. B., *Synthesis,* 341 (1983).
20. Villieras, J., and Rambaud, M., *Synthesis,* 300 (1983).
21. Mouloungui, Z., Delmas, M., and Gaset, A., *Synth. Commun.* **14,** 701 (1984).
22. Garcia-Raso, A., Garcia-Raso, J. A., Campaner, B., Mestres, R., and Sinisterra, J. V., *Synthesis,* 1037 (1982).
23. Sinisterra, J. V., Garcia-Blanco, F., Iglesias, M., and Marinas, J. M., *React. Kinet. Catal. Lett.* **25,** 277 (1984).
24. Frechet, J. M., and Schuert, C., *J. Amer. Chem. Soc.* **93,** 492 (1971).
25. Akhmetov, T. G., *Khim. Prom.* **47,** 711 (1971); *Chem. Abstr.* **75,** 131, 197r (1971).
26. Burriel, F., and Garcia-Clavel, M. E., *An. Fis. Quim.* **57B,** 111 (1961).
27. Judd, M. J., and Pope, M. I., *J. Therm. Anal.* **3,** 397 (1971).
28. Michaud, M., *Rev. Chim. Miner.* **5,** 89 (1968).
29. Michaud, M., *C. R. Acad. Sci. Paris Ser. C* **262,** 1143 (1966).
30. Habashy, G. M., and Kolta, G. A., *J. Inorg. Nucl. Chem.* **34,** 57 (1972).
31. Krishnamurt, D., *Proc. Indian Acad. Sci. A* **50,** 223 (1959).
32. Busing, W. R., and Morgan, H. W., *J. Chem. Phys.* **28,** 998 (1958).
33. Benesi, H. A., *J. Chem. Phys.* **30,** 852 (1958).
34. Thiel, M. V., Becker, E. C., and Pimental, G. C., *J. Chem. Phys.* **27,** 486 (1957).
35. Waldron, R. D., *J. Chem. Phys.* **26,** 809 (1957).
36. Lutz, H. D., Eckers, W., Schneider, G., and Haguseler, H., *Spectrochim. Acta* **37,** 561 (1981).
37. Nakamoto, K., Margoshes, M., and Rundle, R. E., *J. Amer. Chem. Soc.* **77,** 6480 (1955).
38. Miller, F. A., and Wilkins, C. H., *Anal. Chem.* **24,** 1253 (1952).
39. Hunt, J. M., Wisherd, M. P., and Banhan, L. C., *Anal. Chem.* **22,** 1978 (1950).
40. 26-155 card JPCDS Pennsylvania, 1983.
41. 21-073 card JPCDS Pennsylvania, 1983.
42. 21-72 and 22-1054 cards JPCDS Pennsylvania, 1983.
43. 26-154 card JPCDS Pennsylvania, 1983.
44. Manohar, H., and Ramasesnam, S., *Curr. Sci. (India)* **32,** 248 (1963); *Chem. Abstr.* **69,** 8212a (1963); *Z. Krist.* **119,** 357 (1964).
45. Bärnighausen, H., *Anorg. Alg. Chem.* **342,** 233 (1966).
46. Grueninger, H. W., and Bärnigausen, H., *Z. Anorg. Alg. Chem.* **368,** 53 (1968).
47. Yamanaka, T., and Tanabe, K., *J. Phys. Chem.* **80,** 1723 (1976).
48. Tanabe, K., and Saito, K., *J. Catal.* **35,** 247 (1974).
49. Fuentes, A., and Sinisterra, J. V., *Tetrahedron Lett.* **27,** 2967 (1986).
50. Mouloungui, Z., Ph.D. thesis, I.N.P. Toulouse, March 1987.
51. Sinisterra, J. V., Alcantara, A., and Marinas, J. M., *J. Colloid Interface Sci.* **115,** 520 (1987).
52. Jungle, H., and Musso, H., *Spectrochim. Acta A* **24,** 1219 (1968).
53. Bottin-Strzalko, T., Corset, J., Fromet, F., Pouet, M. J., Seyden-Penne, J., and Simonnin, P., *J. Org. Chem.* **45,** 1270 (1980).
54. Strzalko, T., Seyden-Penne, J., Fromet, F., Corset, J., and Simonnin, M. P., *J. Chem. Soc. Perkin Trans. 2,* 783 (1987).
55. Kirilov, M., and Petrov, E., *Chem. Ber.* **104,** 3073 (1971).